

High-Speed Evanescently Coupled Waveguide Type-II UTC Photodiode Under Zero-Bias

Fengxin Yu, Keye Sun, Qianhuan Yu, and Andreas Beling

Department of Electrical and Computer Engineering, University of Virginia, Charlottesville, VA 22904 USA
 Fy6uq@virginia.edu

Abstract: We demonstrate GaAs_{0.5}Sb_{0.5}/In_{0.53}Al_yGa_{0.47-y}As uni-traveling carrier (UTC) waveguide photodiodes with high bandwidth of up to 66 GHz at zero bias and over 100 GHz bandwidth under low bias condition.

OCIS codes: (230.5170) Photodiodes, (060.5625) Radio frequency photonics

1. Introduction

As key components in photonic millimeter-wave wireless communication system and many other microwave photonics applications, photodiodes with large bandwidth and high responsivity are required [1]. Waveguide photodiodes that can be operated at zero bias are particularly beneficial since they reduce energy dissipation on chip and alleviate the electrical cross-talk that occurs with tight metal wiring in dense photonic integrated circuits [2]. In addition, zero-bias photodiodes require no power supply and have small footprint since they do not have bulky bias circuits.

In general, downscaling the photodiode’s dimensions including the absorber thickness, depletion width, and the device active area is an effective way to improve the speed of a photodiode (PD), since it decreases the carrier transit time and the resistance-capacitance (RC) time constant [3]. However, in heterojunction PDs another bandwidth limitation often arises from discontinuities in the band diagram which can impede carrier transport at low and zero bias. In particular, to avoid the potential barrier in the conduction band between the absorber and the wide-bandgap drift layer in an uni-traveling carrier (UTC) PD, a staggered band lineup (type II) is beneficial [4]. Previously, back-illuminated type-II UTC PDs with excellent 3-dB bandwidth of over 140 GHz at zero bias have been demonstrated [5]. However, high-speed surface-normal illuminated PDs usually sacrifice responsivity owing to the thin absorber thickness.

In this work, we designed and fabricated evanescently coupled waveguide type II UTC PDs with dual-integrated waveguide-depletion layer that can achieve high efficiency and high speed simultaneously. A bandwidth of 66 GHz under zero-bias operation and 102 GHz bandwidth at -1 V have been successfully demonstrated for a PD with an active area of 4×4 μm². Larger PDs (5×7 μm²) have 56 GHz bandwidth and an internal responsivity of 0.48 A/W at 0 V.

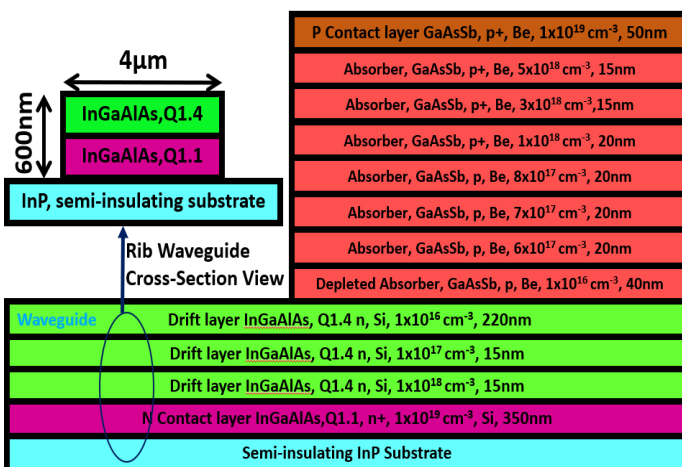


Figure 1. Epitaxial structure of the waveguide PD. All layers are lattice-matched to InP.

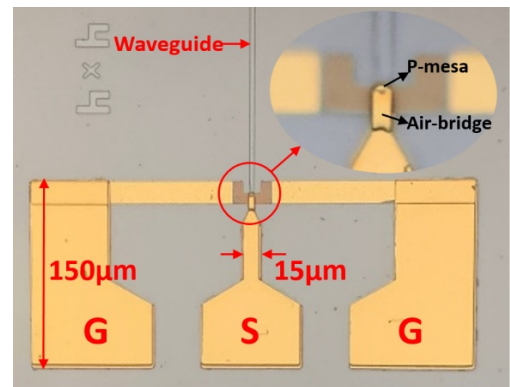


Figure 2. Top-view of a fabricated waveguide PD with ground (G)-signal (S)-ground (G) probe pad.

2. Design and Fabrication

The epitaxial layer structure of the waveguide PD is shown in Figure 1. In order to achieve high efficiency, we utilized an $\text{In}_x\text{Al}_y\text{Ga}_{1-x-y}\text{As}$ dual-integrated waveguide-depletion layer. In this design, the core layer of the passive feeding waveguide serves simultaneously as the electron drift layer in the PD which facilitates efficient light coupling from the waveguide into the absorber over a short length [6]. For the waveguide core layer we used $\text{In}_{0.53}\text{Al}_{0.09}\text{Ga}_{0.38}\text{As}$ which has a higher refractive index than the highly doped n-contact layer to ensure that the optical mode is mostly confined in regions with lower doping. In order to provide high bandwidth under zero bias operation, we used $\text{GaAs}_{0.5}\text{Sb}_{0.5}$ as the absorption layer which results in type II band alignment at the interface to the drift layer. In contrast to the InGaAs/InP MUTC PD in ref. [7], our structure does not require bandgap grading layers since photogenerated electrons are readily injected from the absorber into the drift layer. The epitaxial structure was grown on semi-insulating InP and includes a 250 nm-thick $\text{In}_{0.53}\text{Al}_{0.09}\text{Ga}_{0.38}\text{As}$ drift layer that is lightly graded doped for space-charge compensation and a 150 nm-thick graded doped $\text{GaAs}_{0.5}\text{Sb}_{0.5}$ absorber layer. The doping concentrations of the p-type $\text{GaAs}_{0.5}\text{Sb}_{0.5}$ absorber layer ($5 \times 10^{18} \text{ cm}^{-3}$ - $1 \times 10^{16} \text{ cm}^{-3}$) and the $\text{In}_{0.53}\text{Al}_{0.09}\text{Ga}_{0.38}\text{As}$ drift layer ($1 \times 10^{16} \text{ cm}^{-3}$ - $1 \times 10^{18} \text{ cm}^{-3}$) were carefully designed to create a built-in electric field for electron acceleration in the absorber and a sufficiently large field for high electron velocity in the drift layer, respectively. A double mesa etching process was used to fabricate waveguide PDs. First, the p-mesa and the 4 μm -wide rib waveguide were etched. Then the n-mesa was formed by dry etching and the waveguide regions were etched down to the $\text{In}_{0.53}\text{Al}_{0.09}\text{Ga}_{0.38}\text{As}$ drift layer. $\text{AuGe}/\text{Ni}/\text{Au}$ and $\text{Ti}/\text{Pt}/\text{Au}$ were used for n-metal and p-metal contacts, respectively. The PDs were connected to gold-plated coplanar waveguide radio frequency (RF) pads through an air-bridge. After fabrication, the completed wafer was cleaved to expose the waveguide facets for light input coupling. Figure 2 shows a top-view of a waveguide PD with $16 \mu\text{m}^2$ active area.

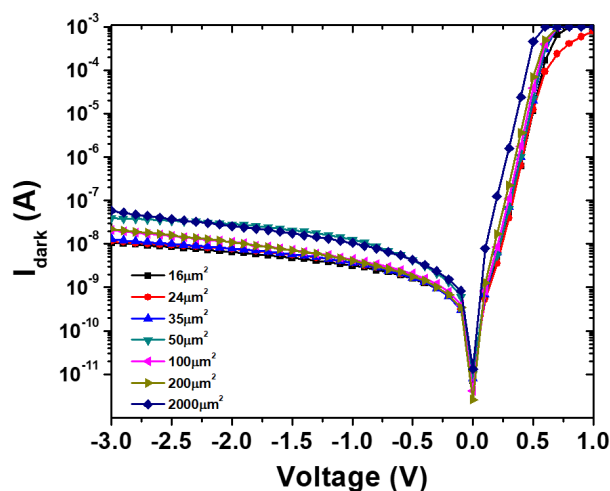


Figure 3. Measured dark currents of waveguide PDs with different active areas.

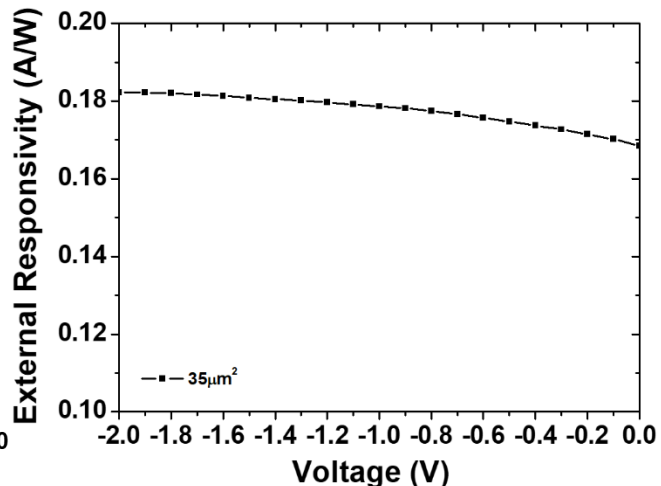


Figure 4. Measured external responsivity at 1550 nm versus reverse voltage of $5 \times 7 \mu\text{m}^2$ waveguide PD.

3. Experimental Results

We measured the I-V characteristics of PDs with different active areas. Figure 3 shows typical I-V curves with dark currents below 100 nA at 3 V reverse bias. The responsivity was measured at 1550 nm wavelength as a function of bias. Figure 4 shows the external (fiber-coupled) responsivity of a $5 \times 7 \mu\text{m}^2$ PD indicating 0.17 A/W at 0 V. We found that the responsivity of our waveguide PD has very small variations when the voltage changes from zero to -2 V (0.17 A/W vs. 0.18 A/W) indicating that the built-in electric field is sufficiently large to collect all photogenerated carriers. In order to determine the internal responsivity, the coupling loss between the tapered fiber and the waveguide was calculated using Beamprop software. After taking into account 3 dB for coupling and 1.5 dB for reflection losses at the waveguide facet, the internal responsivity is estimated to be as high as 0.48 A/W. An optical heterodyne setup with an optical modulation depth close to 100 % was used to characterize the bandwidth. As shown in fig. 5, the RF response was measured at 1 mA average photocurrent. Waveguide photodiodes with active areas of $4 \times 4 \mu\text{m}^2$, 5×7

μm^2 , $5 \times 10 \mu\text{m}^2$ and $5 \times 20 \mu\text{m}^2$ had bandwidths of 66 GHz, 56 GHz, 51 GHz and 41 GHz under zero-bias operation, respectively. When a -1 V bias was applied to the $16 \mu\text{m}^2$ PD, the 3-dB bandwidth was further improved to 102 GHz. Figure 6 shows the bias dependence of the bandwidth for a $5 \times 10 \mu\text{m}^2$ PD at 2 mA. For this device we find that there is only a small roll-off in bandwidth of 20 % below 0.5 V reverse bias. When applying higher reverse bias, the bandwidth becomes flat at 65 GHz. The fact that we observe very little bandwidth dependence with bias indicates that the drift layer is nearly fully depleted under zero bias operation which strongly supports the high speed performance of our PDs.

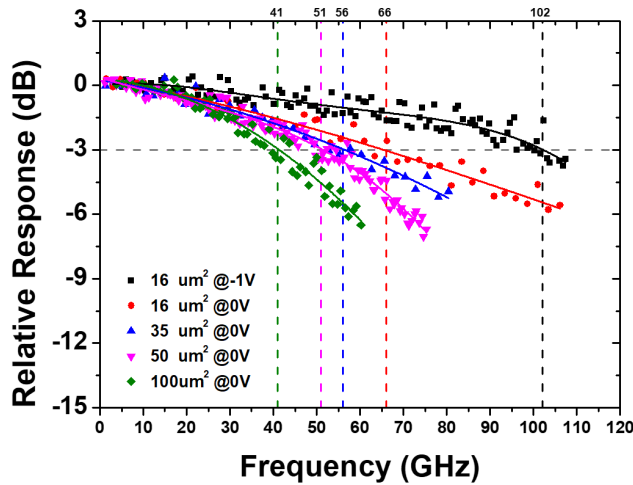


Figure 5. Measured bandwidths of waveguide PDs with different active areas at 1 mA.

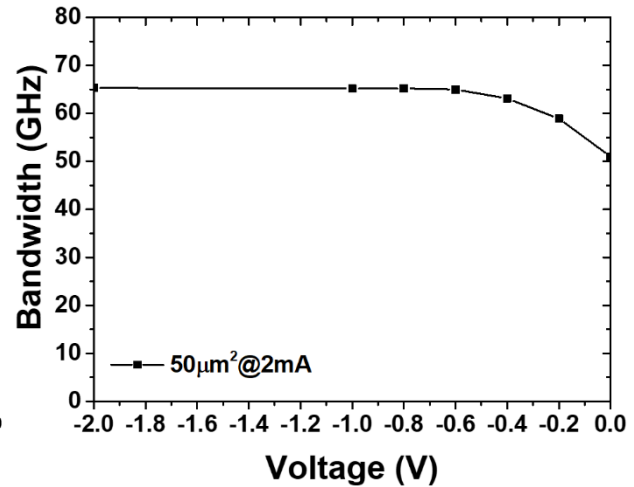


Figure 6. Measured bandwidth of $50 \mu\text{m}^2$ PD at 2 mA.

4. Summary

High-speed evanescently coupled waveguide type-II UTC photodiodes have been successfully fabricated and characterized. The devices do not require a power supply and have high responsivity and high bandwidths of up to 66 GHz.

The authors acknowledge support through the Multidisciplinary University Research Initiative (MURI) program through the Air Force Office of Scientific Research (AFOSR), contract No.FA 9550-17-1-0071, monitored by Dr. Gernot S. Pomrenke.

5. References

- [1] Ishibashi, Tadao, et al. "Unitraveling-carrier photodiodes for terahertz applications." *IEEE Journal of Selected Topics in Quantum Electronics* 20.6 (2014): 79-88.
- [2] Umezawa, T., et al. "Zero-bias operational ultra-broadband UTC-PD above 110 GHz for high symbol rate PD-array in high-density photonic integration." *2015 Optical Fiber Communications Conference and Exhibition (OFC)*. IEEE, 2015.
- [3] Li, Jin, et al. "Analysis of frequency response of high power MUTC photodiodes based on photocurrent-dependent equivalent circuit model." *Optics express* 23.17 (2015): 21615-21623.
- [4] Zheng, Liguang, et al., "Demonstration of high-speed staggered lineup GaAsSb-InP unitraveling carrier photodiodes," in *IEEE Photonics Technology Letters*, vol. 17, no. 3, pp. 651-653, March 2005.
- [5] Wun, Jhih-Min, et al. "Type-II GaAs0.5Sb0.5/InP uni-traveling carrier photodiodes with sub-terahertz bandwidth and high-power performance under zero-bias operation." *Journal of Lightwave Technology* 35.4 (2016): 711-716.
- [6] Tossoun, Bassem, et al. "Ultra-Low Capacitance, High-Speed Integrated Waveguide Photodiodes on InP." *Integrated Photonics Research, Silicon and Nanophotonics*. Optical Society of America, 2019.
- [7] Li, Zhi, et al. "High-saturation-current modified uni-traveling-carrier photodiode with cliff layer." *IEEE Journal of Quantum Electronics* 46.5 (2010): 626-632.